DOI: https://doi.org/10.52756/ijerr.2023.v33spl.006 ***Int. J. Exp. Res. Rev.*, Vol. 33: 57-70 (2023)**

Original Article | *Peer Reviewed* | *Open Access*

International Journal of Experimental Research and Review (IJERR)

ISSN: 2455-4855 (Online)
www.iaph.in
ISSN 2455-4855

An Efficient PV - Integrated UPQC System for Power Quality Enhancement Using Improved Chicken Swarm Optimization

Rudraram Ramesh[1*], Chinnathambi Sasi[1] and Mani Manikandan[2]

[1]Department of Electrical Engineering, Annamalai University, Tamilnadu, India; [2]Department of Electrical and Electronics Engineering, Jyothishmathi Institute of Technology and Science, Karimnagar, Telangana, India

E-mail/Orcid Id:

RR, rameshrudraeee@gmail.com, https://orcid.org/0000-0002-8763-6962; *CS,* saasimeee@gmail.com, https://orcid.org/0000-0001-7254-9033; *MM,* cm.manikandan@gmail.com, https://orcid.org/0000-0002-4881-8157

Article History:
Received: 06th Apr., 2023
Accepted: 19th Sep., 2023
Published: 30th Sep., 2023

Keywords:
PV-UPQC, PQ, series converter, d-q theory, shunt converter, Interleaved Zeta converter, ICS assisted ANFIS MPPT

How to cite this Article:
Rudraram Ramesh, Chinnathambi Sasi and Mani Manikandan (2023). An efficient PV-integrated UPQC system for power quality enhancement using improved Chicken swarm optimization. *International Journal of Experimental Research and Review*. *33*, 57-70.
DOI: https://doi.org/10.52756/ijerr.2023.v33spl.006

Abstract: In today's world, the power distribution system's problems with Power Quality (PQ) are not unfamiliar. However, customer awareness of these issues has also risen. Likewise, there are many conventional solutions to improve the power quality. However, these traditional solutions rely on passive elements and frequently fail to respond effectively as the nature of the power system changes. Custom power devices provide adaptable solutions for many issues. Therefore, a Unified Power Quality Conditioner (UPQC) Coupled with a PV system is proposed in this paper to improve the PQ problems, including fluctuations, voltage sag and swell etc. The deployment of an Interleaved Zeta converter aids in maintaining the constant DC link voltage. In order to derive the maximum desirable power from PV system, STATCOM with Adaptive Neuro- Fuzzy Interference System (ANFIS) is used, which is fine-tuned with the help of the Improved Chicken Swarm (ICS) algorithm. In addition, UPQC with series and shunt converter is employed to decrease the current and voltage harmonics, thereby enhancing the power factor. For controlling the working of UPQC, the d-q theory-based Proportional Integral (PI) is proposed. The suggested design of PV-UPQC is evaluated and the simulation results are obtained in the MATLAB platform with a reduced THD of 2.01%.

Introduction

Increasing the amount of Renewable Energy Sources (RES) penetration in the utility phase has become necessary for utilities due to the rise in electricity consumption, the need to preserve the environment, and the depletion of fossil fuel reserves. Because of their nature and distribution penetration, mitigating environmental pollution, renewable energy can reduce power losses, reduce operating costs, eliminate system upgrades and improve voltage stability. By injecting the RES into the utility grid, the power quality decreases and generates PQ issues (Chawda et al., 2020; Basit et al., 2020). These issues include reactive power flow, voltage fluctuations, excessive neutral current and harmonics etc. Some other problems regarding the voltage side distribution system and RES placement are also discussed by Chang and Chinh (2020). Using a Flexible AC Transmission System (FACTS) largely overcomes these PQ concerns (Khan et al., 2021). The various types of FACT devices mentioned in (Sindi et al., 2023), including Thyristor Controlled Series Compensator (TCSC) controllers, are utilized to improve the quantity of the control flow of active power and transmission lines in electric systems. The Static Var Compensator (SVC) is more effective at supporting the DC voltage and keeps the power supply reliable and efficient (Santika et al., 2018). Static Synchronous Compensator (STATCOM) is an active shunt circuit that improves voltage regulation, power flow, and transmission line stability when connected at the midpoint (Abdelaziz et al., 2020). D-STATCOM is another device which is used for harmonic mitigation and power factor improvement (Saeedinia et

***Corresponding Author:** rameshrudraeee@gmail.com

al., 2022). The distorted voltage is reduced and thus, the power quality improves. The Dynamic Voltage Restorer (DVR) efficiently identifies and rectifies voltage sags in the AC power source by insulating the loads from these power reliability problems (Babu et al., 2021). However, the methods mentioned earlier mostly depend on the control approaches (Babu et al., 2019), which have high power losses. Hence, the proposed PV-UPQC efficiently improves the PQ and grid performance with minimized THD.

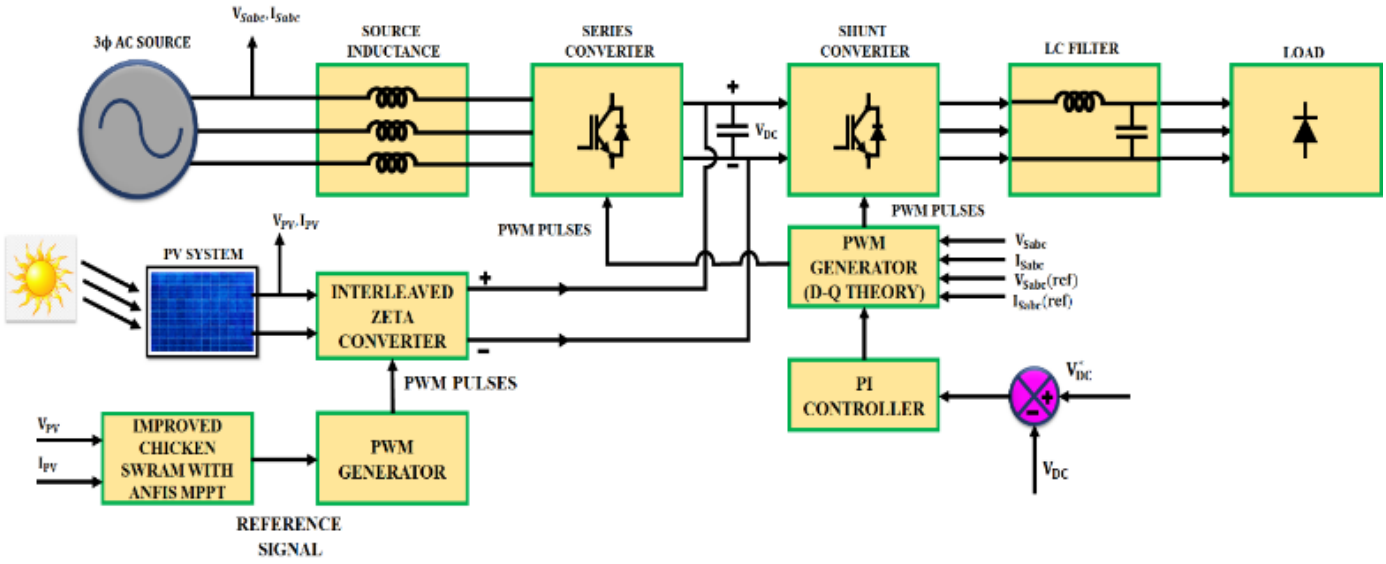

Figure 1. PV-UQPC system configuration

The PV systems are employed to produce the electricity Babu et al. (2021a) to fulfil the load demand. Natural resources could be used to reduce energy consumption. However, a PV array provides a better result, but the output voltage is extremely low (Manikandan et al., 2016; Kumar et al., 2022). Specific types of boost power circuits can control the output voltage. For low power loads, the Boost converter is insufficient. To beat the demerits of the Buck and Boost converter, the combination of Buck-Boost is introduced (Sathish et al., 2022). It is used in industries to step up and down operations. The converter achieves maximum efficiency depending on the conditions and operating modes (Babu et al., 2021b). However, a more comprehensive range of DC input voltage influences the efficiency and generates the ripples.

Moreover, the voltage lift approach-based Luo converter (Reddy et al., 2022a) and SEPIC (Reddy et al., 2022b) enhance PV outputs. However, these converter exhibits issues related to output gains. A non-inverting DC output voltage characterizes the fourth-order Zeta converter (Sathish et al., 2022). But still, due to the high switching losses, the system fails to regulate the gain. The suggested interleaved zeta converter (Sathish et al., 2023) has high efficiency, low input current distortion and less output voltage ripple.

MPPT methods deployed to determine the maximum energy possible from PV systems, have grown in popularity over the last decades. Traditional MPPTs, including incremental conductance and perturb and observe (P & O), are known to be more effective for uniform irradiance with a single peak (Balakishan et al., 2023). Nonetheless, while the system is exposed to Partial Shading (PS) circumstances, it is not applicable and power loss occurs as a result of the algorithm being frequently trapped at a local peak. The Proposed ANFIS extracts the maximum power from PV under PS conditions (Quawi et al., 2023) and the parameters of ANFIS are tuned optimally with the help of the ICS algorithm. This presented approach is effective when compared to other metaheuristic algorithms including Particle Swarm Optimization (PSO) (Rudraram et al., 2023), Whale Optimization (Thota et al., 2023) and Genetic Algorithm (GA) (Abdul et al., 2020).

Therefore, this work proposes a PV integrated with the UPQC system to enhance the PQ issues. The UPQC and series and shunt converter are used to obtain a stabilized output with reduced current harmonics. The proposed ANFIS, tuned with the assistance of ICS, efficiently tracks the utmost power from the PV system. The STATCOM-UQPC is controlled by a PI controller based on the d-q theory. The proposed work is verified using MATLAB simulation.

Proposed System

The control and design of PV-UQPC are suggested in this work. The UQPC Comprises a shunt and series compensator, which is represented in Figure 1.

DOI: https://doi.org/10.52756/ijerr.2023.v33spl.006

A PV-coupled UPQC's primary function is to compensate for PQ issues of the supply voltage, such as sags, unbalance, swells, flicker and harmonics, and load current power quality issues. The Interleaved Zeta converter maintains the stable DC link voltage with reduced ripples. To maximise energy extraction from PV, the PV output is fed into an ICS ANFIS-based MPPT approach, efficiently separating the highest power from PV. By generating gating pulses, the PWM generator regulates the operation of the converter. The converter's controlled outcome of the ideal voltage level is injected into the DC link. The dq theory-based PI controller is employed to control the working of the shunt and series converter of UPQC. As a result, the PQ issues are mitigated with an improved power factor.

Proposed System Modelling

Modelling of PV System

The PV cells are one of the primary components of solar power plants, which convert solar power into electrical energy. Figure 2 depicts the equivalent circuit of a PV cell and its various components. In practical, the resistance R_{sh} and R_s are not included in the system.

The PV cell's output current is

$$I_{PV} = I_L - I_{do} - I_{sh} \text{.....(1)}$$

The diode current equation can be written as,

$$I_{do} = I_o \left\{ \exp\left(\frac{qV_d}{\eta kT}\right) - 1 \right\} \text{.....(2)}$$

The P-V characteristic of the common equation is:

$$I_{PV} = I_L - I_o \left[\exp\left(\frac{q(V_{PV}+IR_s)}{\eta kT}\right) - 1 \right] - \left[V_{PV} + \frac{IR_s}{R_{sh}} \right] \text{.....(3)}$$

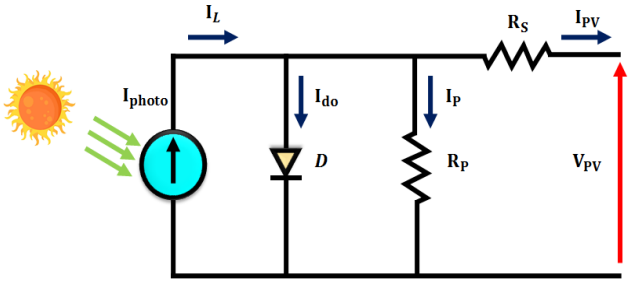

Figure 2. PV Cell

Solar cells can be connected in series or parallel to obtain the desired voltage and current. Furthermore, different connection states result in different photovoltaic array topologies. The output` of PV is severely low. To boost the output voltage and current of PV, the interleaved zeta converter is introduced and it also has high efficiency with a wide range duty ratio.

Modelling of Interleaved Zeta Converter

The traditional converters are frequently used to decrease the DC supply with poor efficiency. However, the conventional Zeta converter is inappropriate for wider-range operations due to its lower efficacy. So, the Interleaved Zeta converter is presented in this work. The Interleaved Zeta Converter's circuit diagram is depicted in Figure 3.

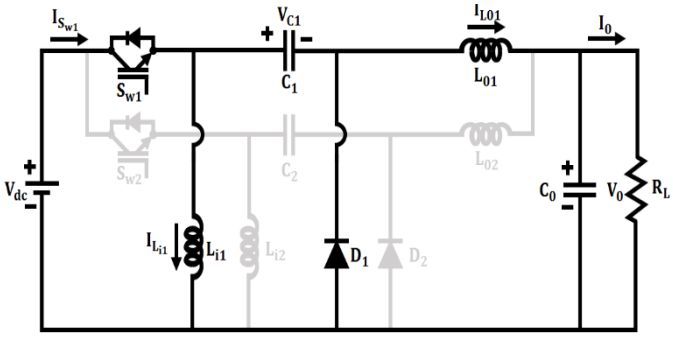

Figure 3. Interleaved Zeta converter circuit diagram

Stage 1 $[t_0 \leq t \leq t_1]$:

The capacitor C_1 and inductor L_{i1}store energy from the DC source V_{dc}. Switch S_1 is switched on during Stage 1, while S_2 is deactivated at the same moment. The output DC connection capacitor C_0 transfers the inductor L_{o1} stored energy to the load. During this mode, the inductors L_{o1} and C_0 are resonating.

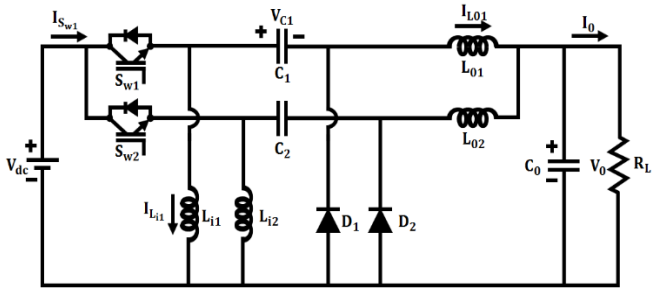

Figure 3. (a). Stage 1

Stage 2$[t_1 \leq t \leq t_2]$:

While in this stage 2, the switches S_1 and S_2 are in ON state. Through the output capacitor C_0, the inductor L_{o1} releases energy to the load. Through the switch S_2 the inductor L_{i2} and C_2 begin charging from the DC source. Towards the end of this mode, the fully charged inductors L_{i1} begin to discharge.

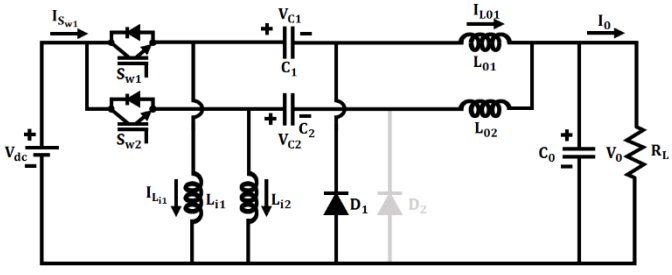

Figure 3(b). Stage 2

Stage 3$[t_2 \leq t \leq t_3]$:

In Stage 3, S_1 is switched off while $S_2$is maintained in the on position. Until the switch is turned on, the inductor L_{i2} and C_2 are continuously charging. Through the DC connection capacitor, the inductors L_{i1} and L_{o1} start discharging to the load. By the end of this phase, L_{o1} is

DOI: https://doi.org/10.52756/ijerr.2023.v33spl.006

fully discharged, charging in the opposite direction, and the output capacitor and load receive the least current.

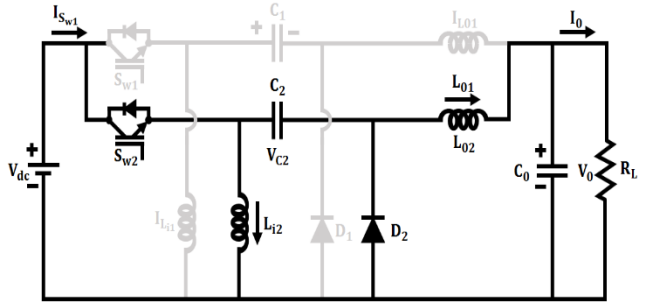

Figure 3(c) Stage 3

Stage 4$[t_3 \leq t \leq t_4]$:

The S_1 and S_2 switches are both switched ON. Through the DC connection capacitor, the inductors L_{i2}, L_{o2} start discharging to the load. Through the switch S_1, the inductors L_{i1},L_{o1} and capacitor C_1 are storing energy from the DC source V_{dc}. The L_{i2}, L_{o2} inductors entirely discharged at the mode's end, and the cycle repeated.

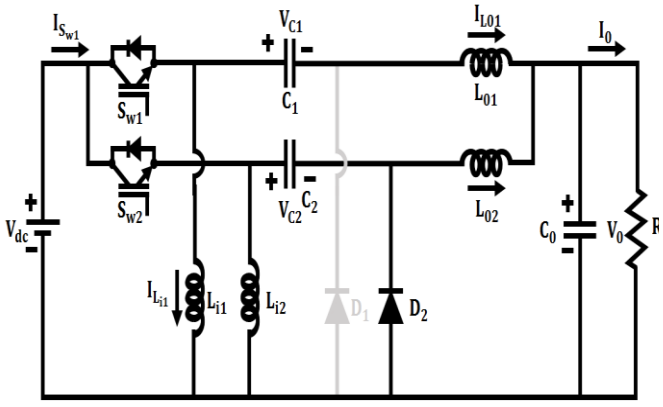

Figure 3(d) Stage 4

The Interleaved Zeta converter ensures optimal power transfer by using an improved CS with ANFIS MPPT controller. The fourth coming section briefly explains suggested ICS-assisted ANFIS MPPT.

Modelling of Improved Chicken Swaram Algorithm with ANFIS MPPT

ANFIS-MPPT

The ANFIS incorporates fuzzy logic with Artificial Neural Network (ANN). An ANN is used to train the new fuzzy controller to determine the variable-based membership function. A comprehensive foundation rule is created by deriving the weight of each node involved (Ahmad et al., 2021). The membership function and rule table can be easily tuned with the aid of the ANN. The ANFIS (Anand et al., 2018) controller's inference system corresponds to a collection of fitness values to optimise nonlinear functions. A two-input (x, y)-one output fuzzy rule set (z) One way to give FIS is as follows:

The first rule states that if x and y are both A_1andB_1, then

$$f_1 = p_1x + q_1y + r_1 \quad \ldots\ldots\ldots\ldots\ldots\ldots (4)$$

The second rule states that if x and y are both A_2andB_2, then

$$f_2 = p_2x + q_2y + r_2 \quad \ldots\ldots\ldots\ldots\ldots\ldots (5)$$

The following equation (6) represents the function of output:

$$f = \frac{\omega_1 f_1 + \omega_2 f_2}{\omega_1 + \omega_2} = \overline{\omega_1} f_1 + \overline{\omega_2} f_2 \quad \ldots\ldots\ldots (6)$$

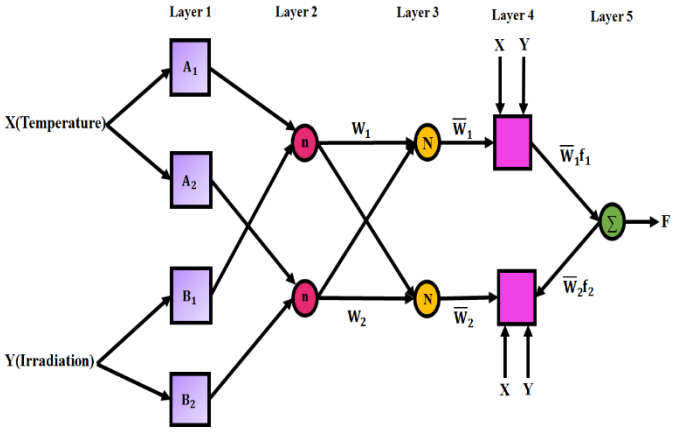

Figure 4. Figure 4. ANFIS based MPPT

Figure 4 depicts the ANFIS's design with two inputs (x, y) and one output (z).

Layer 1

Usually, most nodes are flexible and node i and O_1dependent on the input of the membership functions with corresponding node i for its output.

$$\begin{matrix} O_1,i=\mu_{A_i}(x), & \text{For i=1,2} \\ O_1,i=\mu_{B_i}(y), & \text{For i=3,4} \end{matrix} \quad \ldots\ldots\ldots\ldots\ldots (7)$$

Here, the inputs are x and y, and the corresponding A_i and B_i fuzzy sets are parametric sets of fuzzy sets i. Gaussian membership functions are used for the inputs x and y in this work.

Layer 2

Here, the nodes are unchangeable and output i is the outcome of its input functions. The term "neural network layer" refers to this layer since it multipliers.

$$O_2, i = \omega_i = \mu_{A_i}(x) * \mu_{B_i}(x) \qquad \text{For i} = 1,2 \ldots\ldots\ldots (8)$$

Layer 3

The N fixes and uniquely identifies each node. The output of layer 3 (O_3) i is referred to as having standardised firing strengths from the layer before that since it is the sum of the firing strengths of the rules.

$$O_3, i = \overline{\omega_i} = \frac{\omega_i}{\omega_1 + \omega_2}, \qquad \text{For i} = 1,2 \ldots\ldots\ldots\ldots\ldots\ldots (9)$$

Layer 4

The parameters follow naturally from the changeable node features. This fuzzy logic node has the parameter values p_i,q_i and r_i equation displays the node's output (10)

$$O_4, i = \overline{\omega_i} f_i = \overline{\omega_i}(p_i x + q_i y + r_i), \text{For i} = 1,2 \ldots (10)$$

DOI: https://doi.org/10.52756/ijerr.2023.v33spl.006

Layer 5

It only has one static node, and the sum of all incoming signals is used to calculate its output. Equation illustrates this node's output function (11).

$$O_4, i = \sum_i \overline{\omega_i} f_i = \sum_i \frac{\omega_i f_i}{\sum_i \omega_i}, \text{For } i = 1,2 \ldots\ldots\ldots\ldots\ldots\ldots\ldots (11)$$

An ANFIS's architecture is not a particularly distinctive one; depending on the needs of the application, many levels may be mixed. Through the ANFIS training algorithm, the alterable parameters of the adaptive layers are tuned to match the training dataset results. The solar PV array was simulated in various weather scenarios in the datasets with random temperature and solar irradiance changes. The irradiance G (W/m2) and temperature T (°C) are thus regarded as the ANFIS controller's inputs. The output, which is fed into a duty generator, is the maximum voltage (V_m) produced at any particular time. With the implementation of an efficient improved CS algorithm, the parameters of ANFIS tuned optimally.

Improved CS Algorithm

Initial Selection

The traditional algorithm suffered because the population described in the CS optimisation is not initialised. Additionally, there is no assurance that the algorithm's optimal solution will evenly distribute the search space, which reduces the algorithm's performance and efficiency. The initialization of the algorithm included the chaos method and reverse learning technique. By using the reverse learning strategy, the algorithm's blindness is reduced by making the state non-repetitive and ergodic using the chaotic method. In order to prevent falling into local optimum, the algorithm's ability to detect globally is ensured. The procedure began with the following.

(1) Select the population of chicken swarm optimization $NP_1 = \{x_1(t), x_2(t), \ldots x_N(t)\}$, and the population of every individuals is $x_i(t) = x_{i,1}(t), x_{i,2}(t), \ldots x_{i,D}(t)), i \in N$.

(2) The model iterations produce chaotic and logistic mapping of the equation is described in following equation (12)$NP_2 = \{x_1(t) *, x_2(t) *, \ldots x_N(t) *\}$:

$$x_1(t) *= \mu * x_i(t) * \left(1 - x_i(t)\right), \ldots\ldots\ldots (12)$$

(3) Equation: Determine the inverse solution corresponding to NP_2 individual (13)

$$x_{i,D}(\widetilde{t) = K} * (x_i + y_i) - x_{i,D}(t), \ldots\ldots\ldots\ldots (13)$$

(4) $NP_2 \cup NP_{op}$ and select the best fitness for x_{best} , then compute x_{mean} $(x_1 + x_2 + x_{2N})/2N$ to obtain the inverse optimum solution as shown below.

$$x_{opbest} \begin{cases} x_{best}, & (x_{best}) < f(x_{mean}) \\ x_{mean}, & (x_{best}) \geq f(x_{mean}) \end{cases} \ldots\ldots\ldots (14)$$

The chicken swarm optimisation might locate the ideal solution in a bigger search space by incorporating chaos and reverse learning strategies. It can also direct the individual to develop the ideal solution, improving total convergence speed.

Chicken Location update

It used PSO to determine the position of the particles globally, locally, and locally to optimise the chicks' location update. It chooses the best position for the entire cock-guided group. The particle swarm optimisation algorithm's inertia weight value and learning factor were employed in this study to enhance the chick position updating.

$$x_{i,j}(t+1) = \omega(t) * x_{i,j}(t) + \varphi_1 * \left(x_{m,j}(t) - x_{i,j}(t)\right) + \varphi_2 \left(x_{r,j}(t) - x_{i,j}(t)\right) \ldots\ldots\ldots (15)$$

Wherem is the subgroup member and the person who corresponds to the hen; r is the cock member who corresponds to the chick in the subgroup; φ_1 and φ_2 are earning factors, which, taken together, indicate the extent to which the chick has learned about the hen and the cock; and (t) is weight value.

Setting the Weight Value

The weight value setting impacts the algorithm's ability to do local and global searches, which in turn impacts the algorithm population of diversity in the long run. The nonlinear inertia weight value (t) introduced in this paper is as follows:

$$\omega(t) = \text{floor}\left((\omega_{max} - \omega_{min}) * \exp^3(-2 * (t/T_{max})) + \omega_{min}\right) \ldots\ldots\ldots\ldots\ldots\ldots (16)$$

Where $T_{max}$is the maximum number of iterations, floor is the rounding function, and, where $\omega_{max}$the maximum inertia weight,(t)is an integerω_{min} is the minimum inertia weight..

Settling the learning factor

Similar to the social and individual learning factors in the PSO, the 0 φ_1 and φ_2 in the chick position update show the extent of learning of chicks to cocks and hens derived from the PSO component. It can be inferred that the larger φ_1 is, the higher the probability the chick has to search around the hen at the start of the search, and it is more inclined to search for the globally optimal solution;

DOI: https://doi.org/10.52756/ijerr.2023.v33spl.006

the largerφ_2 , the chick is more likely to find the rooster, which is a local search close to the optimal solution. This Paper implements a nonlinear learning component, enabling local and global searches for chicks. The equation is as follows:

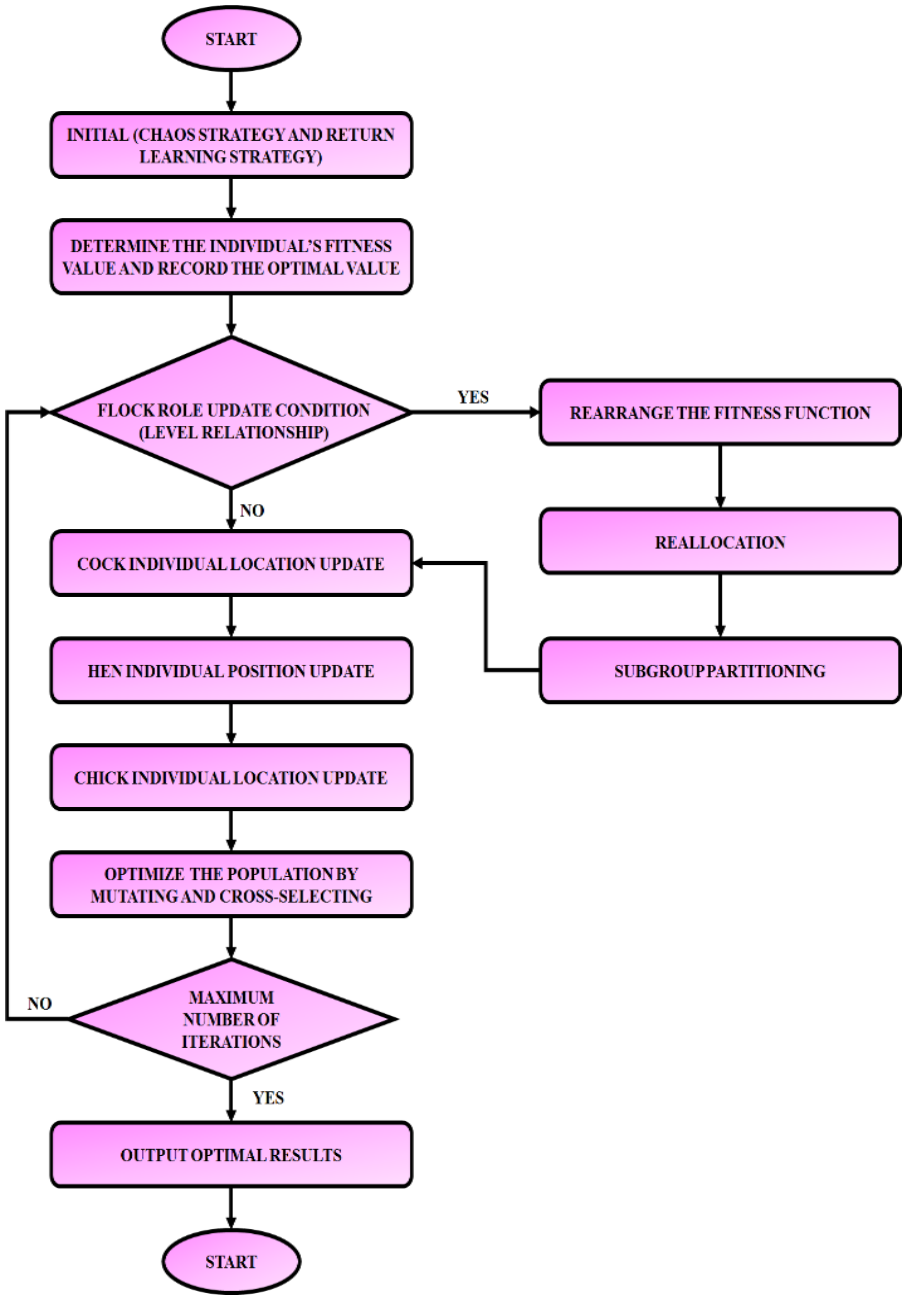

Figure 5. Flow chart of ICS Algorithm

$$\varphi_1 = 1.3 + 1.2 * \cos(t\pi/T_{max}), \quad \ldots\ldots\ldots\ldots (17)$$

$$\varphi_2 = 2 - 1.2 * \cos(t\pi/T_{max}) \ldots\ldots\ldots (18)$$

Select the Best Individual

A differential method that consists of the three stages of variation, intersection, and selection is utilised to choose the best location for the chicken swarm optimisation. The important equation is as follows:

(1) Variation Procedure: Following a random selection of two identical-iteration-number bodies, $x_{r1,j}(t)$and$x_{r2,j}(t)$, the mutation operation is carried out by the following equation.

$$V_{i,j}(t+1) = x_{i,j}(t) + F * \left(x_{r1,j}(t) - x_{r2,j}(t)\right) \ldots. (19)$$

Where F is a random factor which regulates the extent of growth of the score vector and $V_{i,j}(t+1)$ is the mutant individual.

(2) Cross Procedure: Indicator of cross-probability P is added, and the cross operation is carried out using the equation below:

$$k_{i,j}(t) = \begin{cases} v_{i,j}(t+1), & P \in [0,1], \\ x_{i,j}(t), & \text{otherwise} \end{cases} \ldots\ldots\ldots\ldots (20)$$

DOI: https://doi.org/10.52756/ijerr.2023.v33spl.006

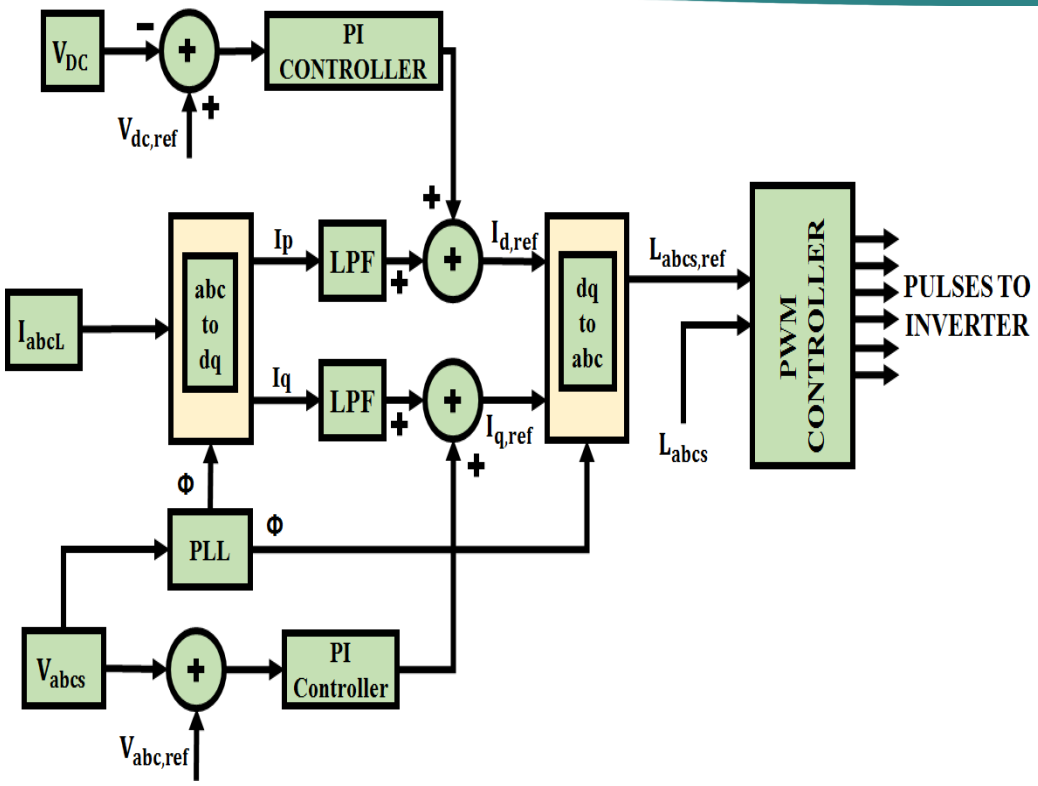

Figure 6. Shunt control approach

(3) Selection Procedure: Choose individuals with high fitness function values, crossover operations and run mutation and compare the new individuals with the previous generation to compare the fitness function values of two individuals. If the former exceeds the latter in size, move on to the next iteration; otherwise, stay the same.

Figure 5 indicates the flow chart representation of the ICS Algorithm. The proposed ICS fine-tuned the parameter with the best optimal solution.

Modelling of UPQC

Generally, the UPQC consists of two main converters: shunt and dc converters. These two converters maintain a common DC link with a renewable energy source, which helps UPQC work to enhance the PQ. The UPQC serves as a power quality mitigation and conditioning device for PV integration. The shunt converter injects current to reduce harmonics caused by nonlinear load. In order to provide and inject voltage in series with line to the distortion-free voltage at the load terminal, the UPQC series converter is used in voltage control mode. Because of its excellent rapid performance and minimal computational effort, a DQ theory-based control, a time domain approach is adopted.

Shunt Control Technique

The improved DQ control technique is shown in Figure 6. The power supply current (I_{sa}, I_{sb}, I_{sc}), power supply voltage (V_{sa}, V_{sb}, V_{sc}), load current ($I_{La,} I_{Lb}, I_{Lc}$), and DC link voltage (V_{dc}) are the first signals sensed in this control approach.

Eventually, change the load current from an abc-frame to a dq-frame using equation (18).

$$\begin{bmatrix} i_d \\ i_q \\ i_o \end{bmatrix} = \frac{2}{3}\begin{bmatrix} \cos\emptyset & -\sin\emptyset\,\frac{1}{2} \\ \cos\left(\emptyset-\frac{2\pi}{3}\right) & -\sin\left(\emptyset-\frac{2\pi}{3}\right)\frac{1}{2} \\ \cos\left(\emptyset+\frac{2\pi}{3}\right) & \sin\left(\emptyset-\frac{2\pi}{3}\right)\frac{1}{2} \end{bmatrix}\begin{bmatrix} i_{la} \\ i_{lb} \\ i_{lc} \end{bmatrix} \quad \ldots. (18)$$

To produce a constant DC component, the filter lets these i_d and i_q components through. The reference current,i_{dref}, is obtained by combining i_{ddc} with the loss component obtained by adjusting the DC link error signal. Equations (19) and (20) provide the loss component and the direct axis reference current.

$$i_{ln} = i_{1(n-1)} + k_{pd}\left(V_{de(n)} - V_{de(n-1)} + k_{id}V_{de(n)}\right) \ldots. (19)$$

$$i_d^* = i_1 + i_{ddc} \quad \ldots\ldots\ldots\ldots\ldots\ldots\ldots\ldots\ldots\ldots\ldots\ldots (20)$$

The reference current i_{qref} is obtained similarly by combining i_{qdc} with the tuning power supply voltage error signal, as illustrated in equation (21). The final reference currents provided by equation are these reference i_{dref} and i_{qref}currents are converted back to the abc-reference system via the inverse Park Transformation (22).

$$i_{qrn} = i_{qr(n-1)} + k_{pq}\left(V_{te(n)} - V_{te(n-1)} + k_{id}V_{te(n)}\right) \ldots (21)$$

DOI: https://doi.org/10.52756/ijerr.2023.v33spl.006

$$i_q^* = i_{qr} + i_{qdc} \quad \ldots\ldots\ldots\ldots\ldots\ldots\ldots\ldots\ldots\ldots\ldots\ldots (22)$$

The PWM controller generates gate pulses based on the difference between the reference source current and the actual source current. Using the flash pulse as a basis, the current injects into the PCC to reduce harmonics and compensate for the necessary reactive power.

Series Control Technique

The series controller aims to lessen voltage sags, surges, and interruptions. Moreover, voltage harmonics are compensated appropriately. In Figure 7, the suggested series voltage controller is displayed. First, transform the source voltage into the synchronous dq0 reference frame using the following equation.

$$V_{s1}^{dq0} = T_s * V_{s1}^{abc} = V_{S1p} + V_{S1n} + V_{S10} + V_{S1h} \quad \ldots. (23)$$

It comprises positive, negative, zero sequence, and harmonic components, respectively, designated as V_{S1p}, V_{S1n}, V_{S10} and V_{S1h}. The load voltage's dq0 reference system is developed to obtain the sinusoidal voltage.

$$V_{L1}^{dq0} = T_s * V_{s1}^{abc} = \begin{bmatrix} U_m \\ 0 \\ 0 \end{bmatrix} \quad \ldots\ldots\ldots\ldots\ldots\ldots\ldots\ldots\ldots\ldots (24)$$

$$\text{Where } Ts = \begin{bmatrix} \cos\emptyset & -\sin\emptyset\frac{1}{2} \\ \cos\left(\emptyset - \frac{2\pi}{3}\right) & -\sin\left(\emptyset - \frac{2\pi}{3}\right)\frac{1}{2} \\ \cos\left(\emptyset + \frac{2\pi}{3}\right) & \sin\left(\emptyset - \frac{2\pi}{3}\right)\frac{1}{2} \end{bmatrix} \quad \ldots\ldots.(25)$$

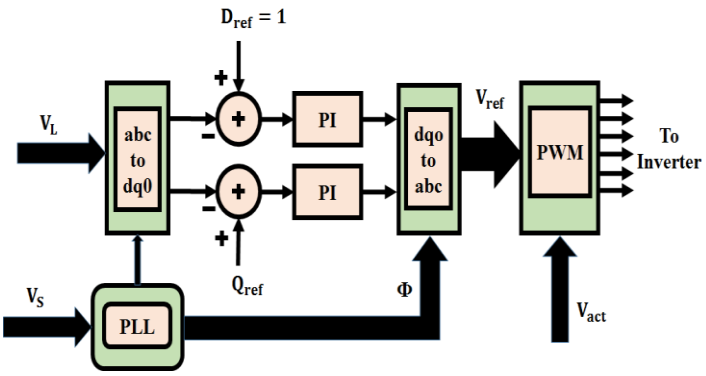

Figure 7. Series control approach

This formula yields the compensation dq0 reference frame voltage:

$$V_{dq0}^{ref} = V_{s1}^{dp0} - V_{L1}^{dp0} \quad \ldots\ldots\ldots\ldots\ldots\ldots\ldots\ldots\ldots\ldots (26)$$

The abc-reference frame continues to be converted from this compensating voltage. Produce gate pulses using PWM to produce compensation for load voltage fluctuations. As a result, an effective ICS with ANFIS MPPT for PV-UPQC system using an Interleaved Zeta converter achieves improved PQ issues.

Results and Discussion

An effective Improved CS optimization is introduced for the PV-UQPC system using the interleaved zeta converter discussed in this work. To deliver the power required by the shunt and series compensation, the PV system is connected to the DC link of UPQC. This part validates the suggested control approach with MATLAB and discusses the outcomes in-depth. Table 1 displays the parameters used to develop the suggested work.

Table 1. Parameter Specification

Parameter	Specification
Solar PV System	
Series connected solar PV cells	36
Open Circuit Voltage	12V
Short Circuit Current	8.33A
Peak Power	10KW, 10 Panels
Interleaved Zeta Converter	
$L_1, L_2, L_3 \& L_4$	$2 * (350uH - 6A) + 2 * (350uH - 2A)$
$C_1, C_2, C_3 \& C_4$	47uF
$C_{o1} \& C_{o2}$	180u
C_{in}	470 uF

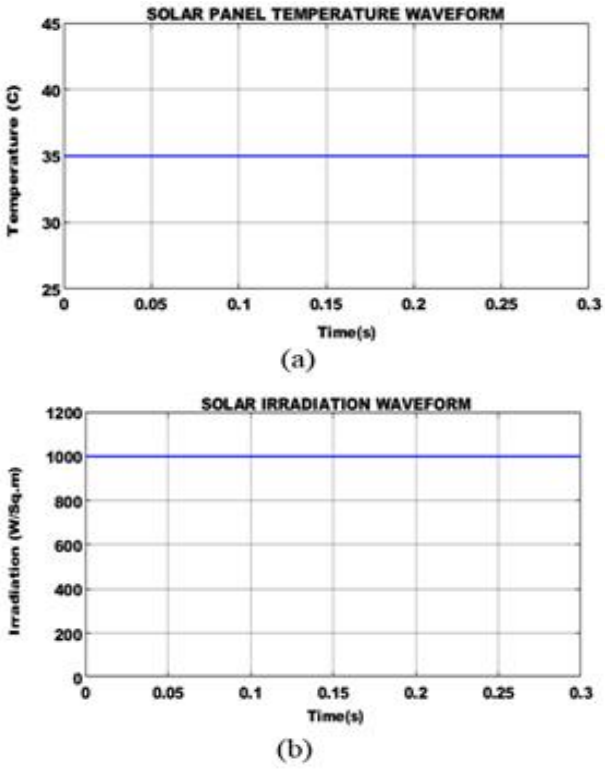

Figure 8. Solar panel (a) Temperature (b) Irradiation

To verify the functionality of the interleaved Zeta converter, a PV system powered by renewable energy is linked to the interleaved converter. It is obvious from the waveform observation in Figure 8(a) that the temperature

DOI: https://doi.org/10.52756/ijerr.2023.v33spl.006

remained constant at 35°C, and this information may be used to analyse the effectiveness of the suggested technique in addressing the intermittent nature of the PV system. Similarly, Figure 8 (b) demonstrates that an irradiation of 1000 W/Sq.m PV system is attained.

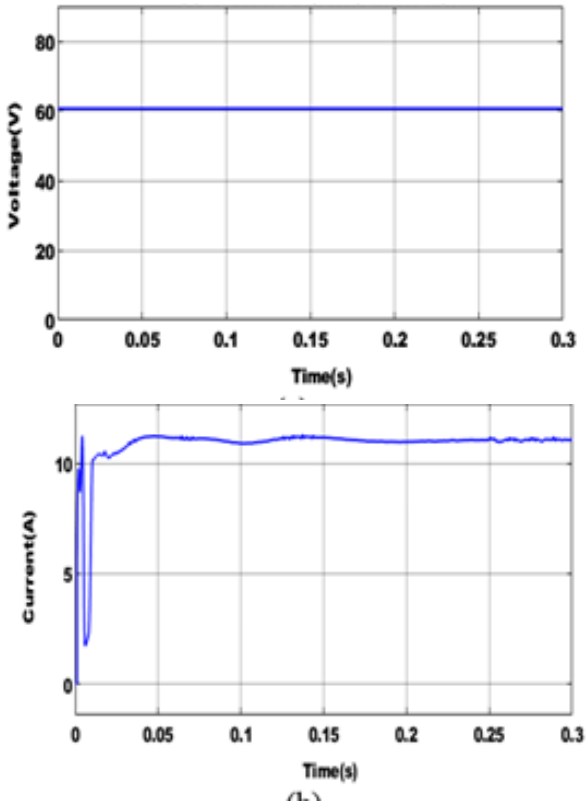

Figure 9. Solar panel (a) Voltage (b) Current

Figure 8 indicates the waveform representation for Voltage and irradiation of PV system. From the graph, it is noted that the constant voltage 60V is maintained. Similarly, the current obtains a peak value and after 0.2 sec it maintains a constant value of 12 A.

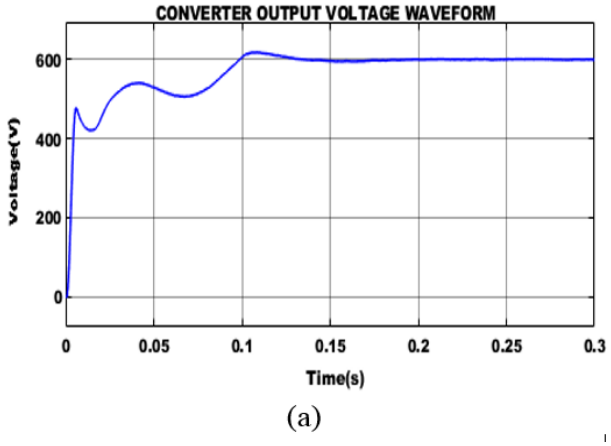

(a)

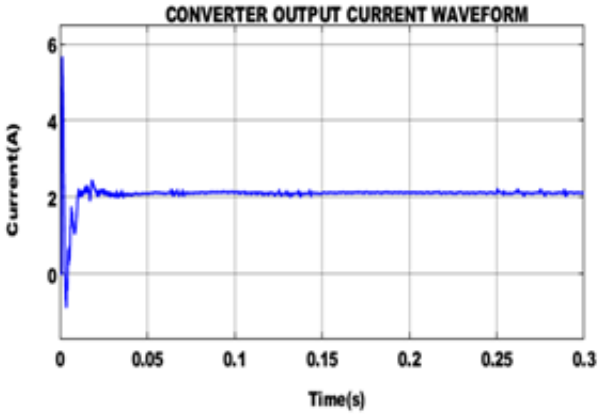

(b)

Figure 10. Output of Interleaved Zeta converter (a) Voltage (b) Current

In Figure 9(a), the waveforms for the Interleaved Zeta converter's voltage output are displayed. The converter's output voltage of 600V is reached in 0.15 seconds, even with some initial variations. The output current is also dynamic in Figure 7(b) until 0.5s, at which point a constant value of 2A is maintained.

Case 1: FOR STEP MAGNITUDE (-0.3)

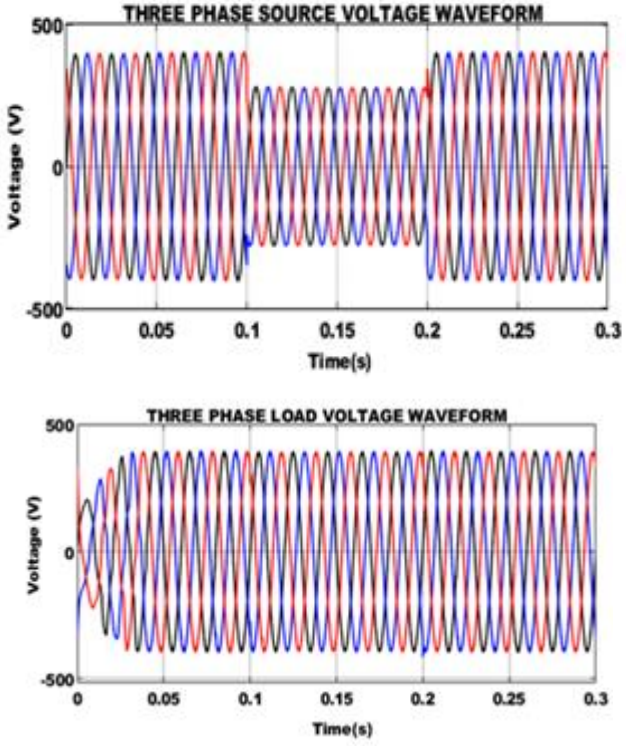

DOI: https://doi.org/10.52756/ijerr.2023.v33spl.006

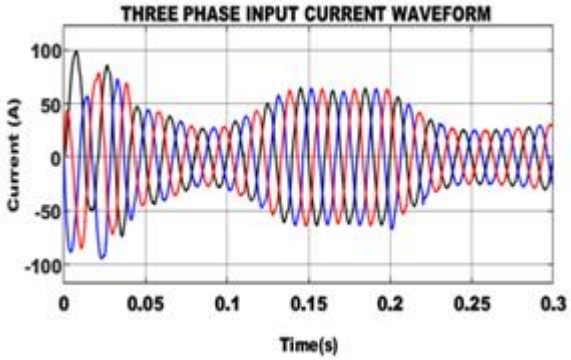

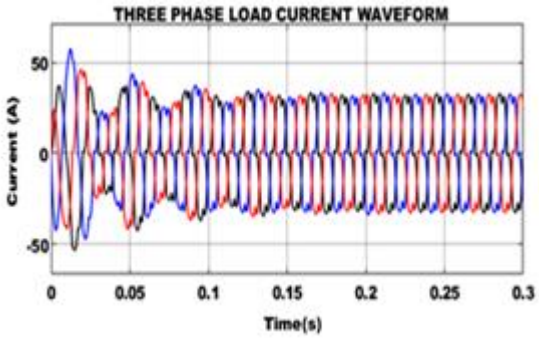

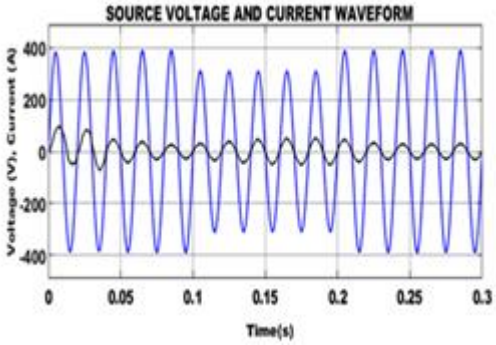

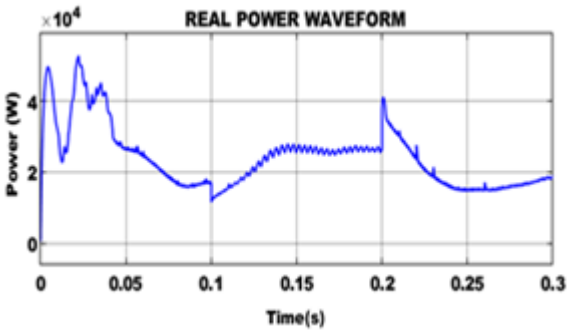

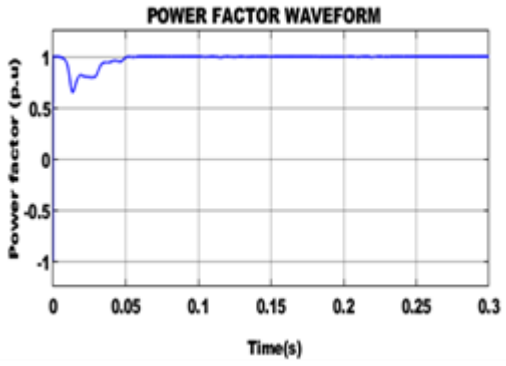

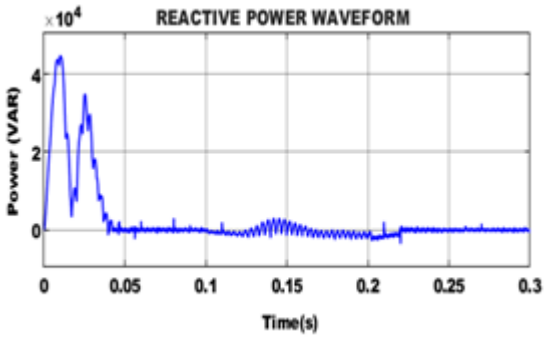

Figure 11. Simulation results for voltage sag condition

Case 1 assesses the feasibility and effectiveness of the proposed PV-UPQC under voltage sag conditions. The source voltage is initially 400V, and between the intervals of 0.1 and 0.2 seconds, a voltage sag of magnitude -0.3 p.u is induced. The input current increases to 55A during this time, as seen in Figure 10. The resulting waveform also shows the analysis of the source current and source voltage under voltage sag by considering into reference a single phase. Moreover, at 0.05 seconds a unity power factor is attained. Due to the robust compensation abilities of the series compensator, the stability of the load side voltage is maintained over the voltage sag in the grid side. The suggested method also successfully reduces reactive power.

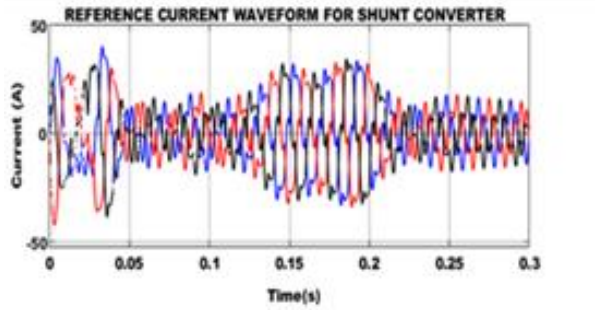

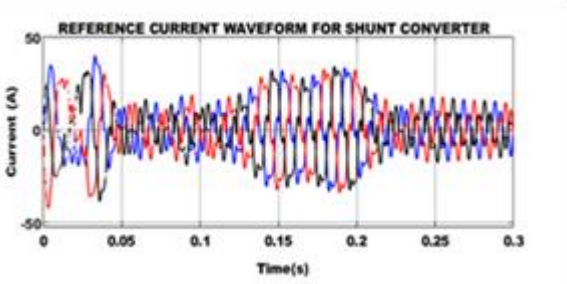

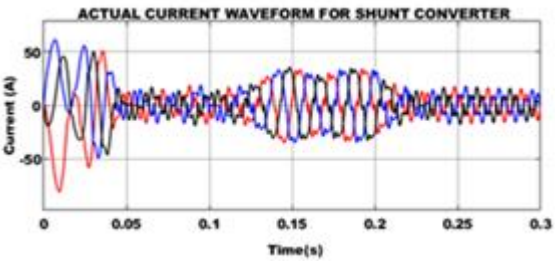

DOI: https://doi.org/10.52756/ijerr.2023.v33spl.006

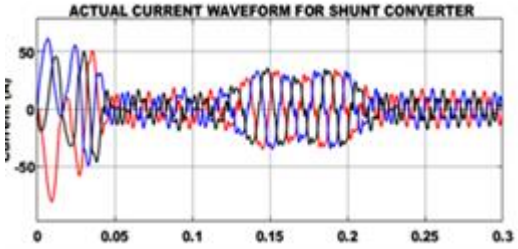

Figure 12. The waveform of shunt and series compensator for voltage sag condition

Figure 11 shows the reference current signal for the shunt compensator that is produced using the PI controller-assisted dq theory. Similarly, the reference voltage for the series compensator signal is produced with the aid of the dq theory. The waveform also shows the actual voltage and current waveforms for the shunt and series compensators. As a result of using the designed PV-UPQC, the system's current and voltage quality issues are rectified.

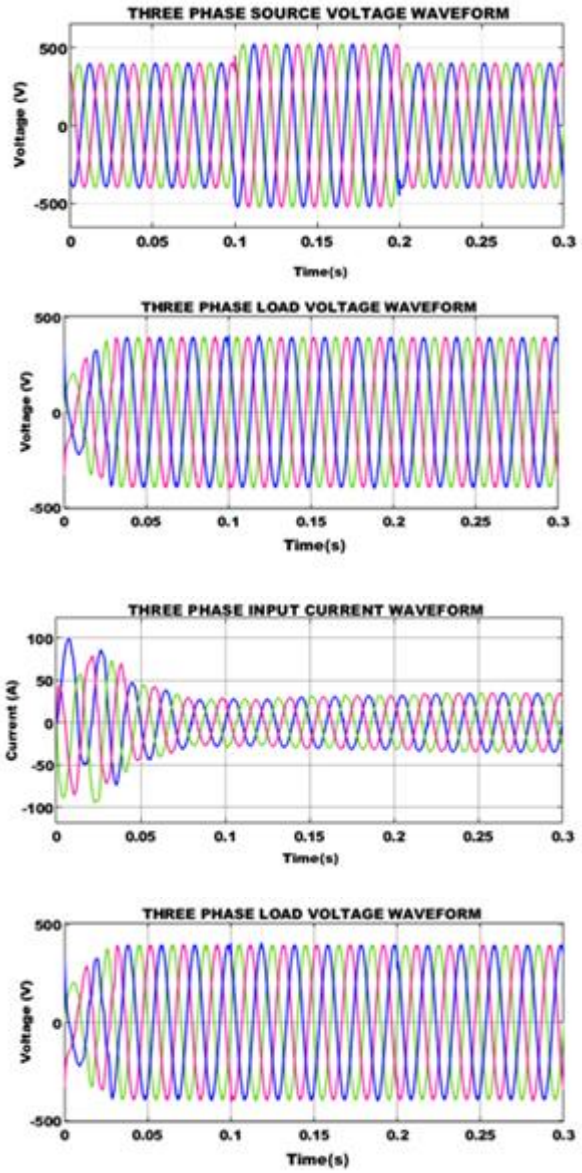

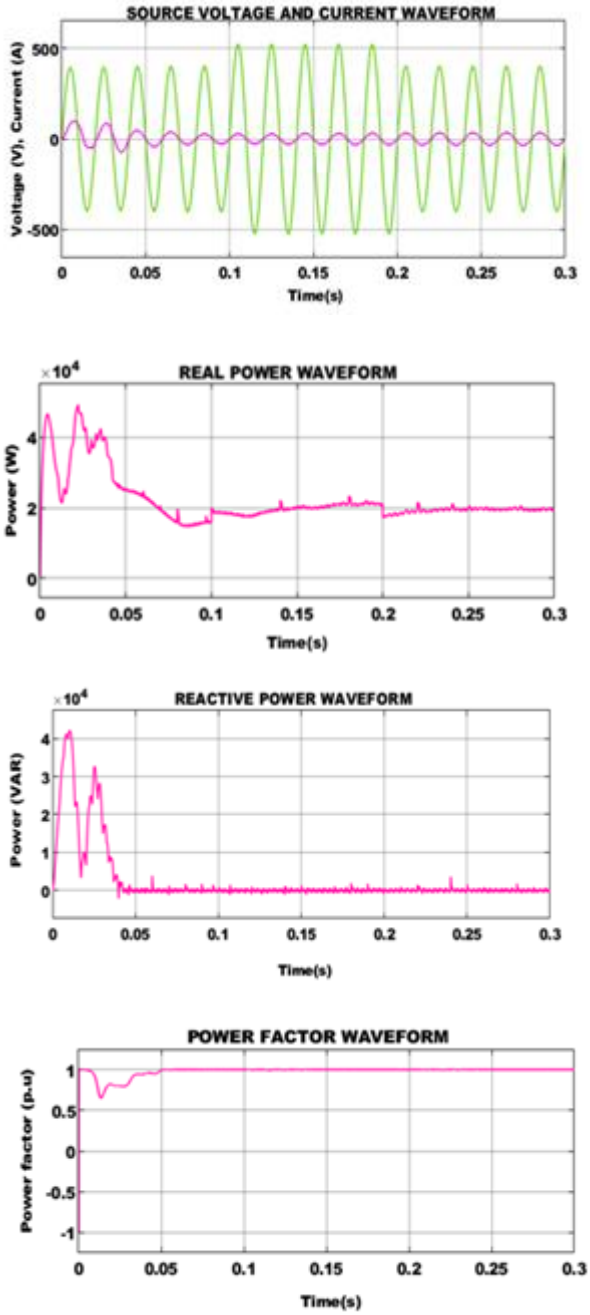

Figure 13. Simulation results for voltage swell condition

Case 2 evaluates the PV-UPQC's dynamic operation in the presence of voltage swell, and Figure 12 shows the relevant waveforms. In case 2, between 0.1 and 0.2 seconds, a voltage swell of magnitude 0.3p.u is seen in the source voltage waveform. The next waveform shows the corresponding input current waveform, in which magnitude decreases in response to the voltage swell. The waveforms for a single phase of the source voltage and current under the voltage swell condition are also considered. Similar to case 1, case 2 a unity power factor is achieved. The excellent compensating capability of the series and shunt compensators of the proposed UPQC enables the maintenance of a constant and stable voltage

DOI: https://doi.org/10.52756/ijerr.2023.v33spl.006

and current on the load side. Figure 12 also displays the real and reactive power waveforms. Figure 13 shows the reference voltage and current waveforms that are used to rectify PQ concerns.

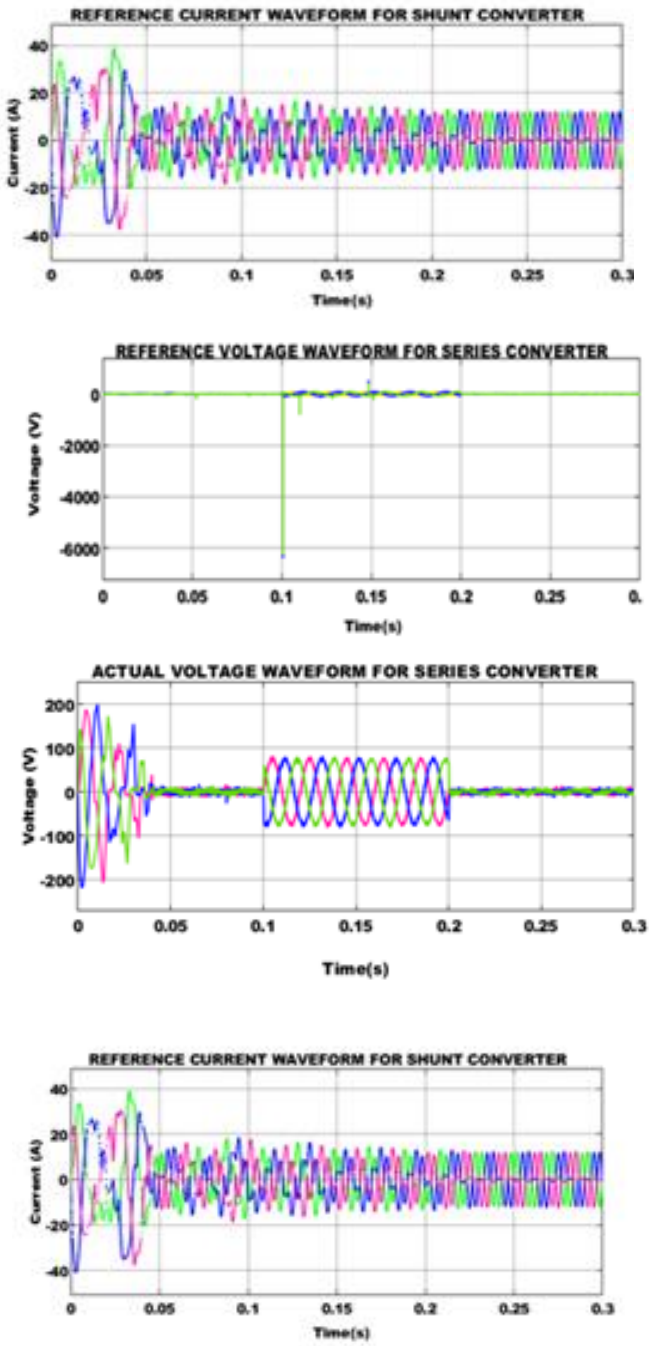

Figure 14. Waveform of shunt and series compensator for voltage swell condition

Figure 15 shows the comparison graphs used to evaluate the effectiveness of DC-DC converters in terms of voltage gain, efficiency, and tracking efficiency. The suggested ICS with ANFIS MPPT has the best efficiency, approximately 96%, compared to other methods. Similarly the THD waveform is seen in Figure 14. The Interleaved Zeta values' voltage gain, efficiency and THD are 1:10, 97.2% and 2.01%, respectively.

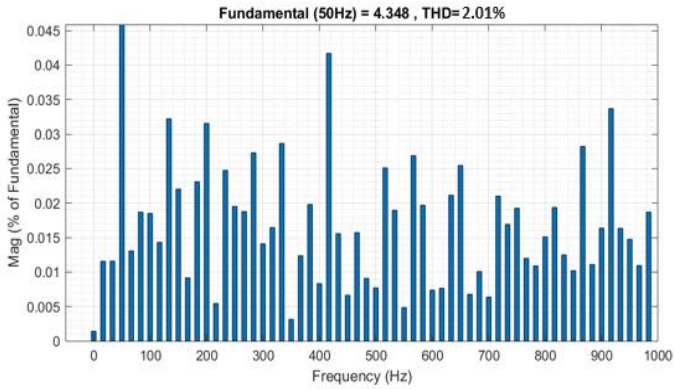

Figure 15. THD Waveform

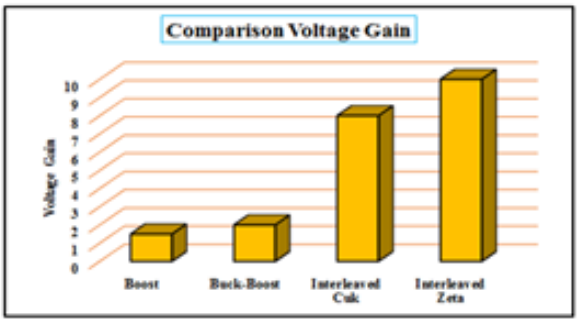

(a)

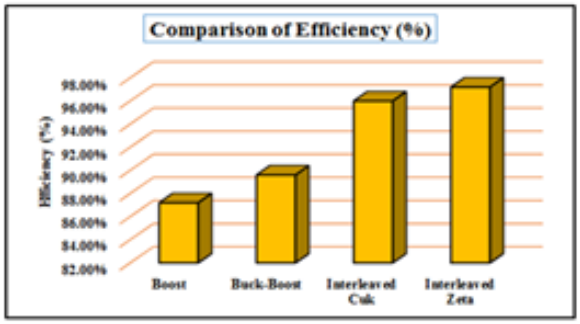

(b)

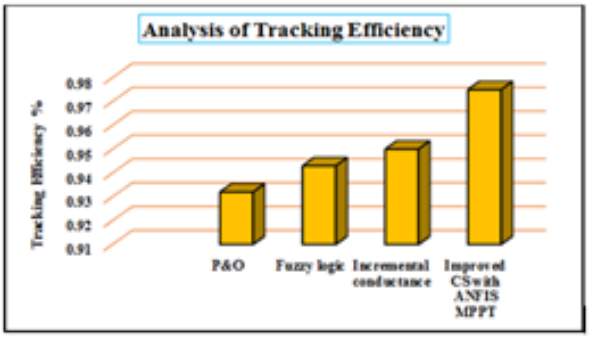

(c)

Conclusion

The RES are crucial to producing the electrical power in grid-coordinated PV systems. Because of the RES connection with the grid, the PQ problems show a drastic increase. Due to this poor power quality, the grid has to deal with load shedding, fluctuations in harmonics, voltage swell & sag and other difficulties that impact the

DOI: https://doi.org/10.52756/ijerr.2023.v33spl.006

system. The PV integrated UPQC is proposed in this work to overcome the issues mentioned earlier. With the help of Interleaved Zeta converter the high ripples are eliminated. In order to track the maximized power from PV, the ANFIS MPPT is introduced, which is effectively tuned by the employment of the improved CS algorithm. The UQPC's series and shunt compensators lessen voltage sag, swell, and harmonics. The coordinated dq theory and PI controller are introduced to enhance the performance of the UPQC system. The proposed PV-UPQC is evaluated and the simulation results are obtained in MATLAB platform. According to the results, the interleaved zeta converter has an outstanding efficiency of 97.2% with minimized THD value of 2.01%.

Acknowledgement

Annamalai University & Jyothishmathi Institute of Technology and Science provided the laboratory facilities and support for this study, which the authors gratefully acknowledge. The Departments of Higher Education, Science and Technology are all acknowledged by the authors. Annamalai University's support in carrying out this research work.

Conflict of Interest

Nil

References

Abdelaziz, S., Kamel, C., & Saad, K. (2020). Multiphase Interleaved Bidirectional DC-DC Converter for Electric Vehicles and Smart Grid Applications. *International Journal of Smart Grid –Smart Grid*, *4*(2), 80-87.

Abdul, R.A. (2020). Solar PV System for Water Pumping Incorporating an MPPT based Bat Optimization Circuits and Systems. *Journal of Advanced Research in Dynamical and Control Systems*, *12*(01-Spl. Issue), 786- 794. https://doi.org/10.5373/JARDCS/V12SP1/20201130

Ahmad, M.W., Gorla, N.B.Y., Malik, H., & Panda, S.K. (2021). A Fault Diagnosis and Postfault Reconfiguration Scheme for Interleaved Boost Converter in PV-Based System.*IEEE Transactions on Power Electronics*, *36*(4), 3769-3780. https://doi.org/10.1109/TPEL.2020.3018540

Anand, I., Senthilkumar, S., Biswas, D., & Kaliamoorthy, M. (2018). Dynamic Power Management System Employing a Single-Stage Power Converter for Standalone Solar PV Applications. *IEEE Transactions on Power Electronics*, *33*(12), 10352-10362. https://doi.org/10.1109/TPEL.2018.2804658

Babu, V., Ahmed, K.S., & Shuaib, Y.M. (2021a). A novel intrinsic space vector transformation based solar fed dynamic voltage restorer for power quality improvement in distribution system. *J. Ambient Intell Human Comput*, 2021. https://doi.org/10.1007/s12652-020-02831-0

Babu, V., Ahmed, K.S., Shuaib, Y.M., & Manikandan M. (2021b). Power Quality Enhancement Using Dynamic Voltage Restorer (DVR)-Based Predictive Space Vector Transformation (PSVT) With Proportional Resonant (PR)-Controller. *IEEE Access*, *9*, 155380-155392. https://doi.org/10.1109/ACCESS.2021.3129096

Babu, V., Basha, S.S., Shuaib, Y.M., Manikandan, M., & Enayathali, S.S. (2019). A novel integration of solar fed dynamic voltage restorer for compensating sag and swell voltage in distribution system using enhanced space vector pulse width modulation (ESVPWM). *Universal Journal of Electrical and Electronic Engineering*, *6*(5), 329-350. https://doi.org/10.13189/ujeee.2019.060504

Balakishan, P., Chidambaram, I.A., & Manikandan, M. (2023). An ANN Based MPPT for Power Monitoring in Smart Grid using Interleaved Boost Converter. *Tehnički Vjesnik*, *2*(30), 381-389. https://doi.org/10.17559/TV-20220820194302

Basit, M.A., Dilshad, S., Badar, R., & Rehman, S.M.S. (2020). Limitations, challenges, and solution approaches in grid-connected renewable energy systems. *International Journal of Energy Research*, *44*(6), 4132-4162. https://doi.org/10.1002/er.5033

Chang, G.W., & Chinh, N.C. (2020). Coyote optimization algorithm-based approach for strategic planning of photovoltaic distributed generation. *IEEE Access*, *8*, 36180-36190. https://doi.org/10.1109/ACCESS.2020.2975107

Chawda, G.S., Shaik, A.G., Mahela, O.P., Padmanaban, S., & Nielsen, J.B.H. (2020). Comprehensive Review of Distributed FACTS Control Algorithms for Power Quality Enhancement in Utility Grid With Renewable Energy Penetration. *IEEE Access*, *8*, 107614-107634. https://doi.org/10.1109/ACCESS.2020.3000931

Khan, N.H., Wang,Y., Tian, D., Jamal, R., Iqbal, S., Saif, M.A.A., & Ebeed, M. (2021). A novel modified lightning attachment procedure optimization technique for optimal allocation of the FACTS devices in power systems. *IEEE Access*, *9*, 47976-47997. https://doi.org/10.1109/ACCESS.2021.3059201

Kumar, T.P., Ganapathy, S., & Manikandan, M. (2022). Improvement of voltage stability for grid connected solar photovoltaic systems using static synchronous compensator with recurrent neural network. *Electrical Engineering & Electromechanics*, *2*, 69-77. https://doi.org/10.20998/2074-272X.2022.2.10

Manikandan, M., & Basha, A.M. (2016). ODFF: Optimized Dual Fuzzy Flow Controller Based Voltage Sag Compensation for SMES-Based DVR in Power Quality Applications. *Circuits and Systems*, 7(10), 2959-2974. https://doi.org/10.4236/cs.2016.710254

Reddy, S.G., Ganapathy, S., & Manikandan, M. (2022a). Three Phase Four Switch Inverter Based DVR for Power Quality Improvement With Optimized CSA Approach. *IEEE Access*, *10*, 72263-72278. doi: https://doi.org/10.1109/ACCESS.2022.3188629

Reddy, S.G., Ganapathy, S., & Manikandan, M. (2022b). Power quality improvement in distribution system based on dynamic voltage restorer using PI tuned fuzzy logic controller, *Electrical Engineering & Electromechanics*, *1*, 44-50. https://doi.org/10.20998/2074-272X.2022.1.06

Rudraram, R., Chinnathambi, S., & Mani, M. (2023). PV Integrated UPQC with Intelligent Control Techniques for Power Quality Enhancement. *International Journal of Electrical and Electronics Research* (IJEER), *1*(11), 202-212. https://doi.org/10.37391/ijeer.110128

Saeedinia, S., Shamsi-Nejad, M.A., & Eliasi, H. (2022). A two-stage grid-connected single-phase SEPIC-based micro-inverter with high efficiency and long lifetime for photovoltaic systems application. *Iranian Journal of Electrical and Electronic Engineering*, *18*(2), 2355. https://doi.org/10.22068/IJEEE.18.2.2355

Santika, W.G., Urmee, T., Anissuzaman, M., Shafiullah, G.M., & Bahri, P.A. (2018). Sustainable energy for all: Impacts of Sustainable Development Goals implementation on household sector energy demand in Indonesia. *International Conference on Smart Green Technology in Electrical and Information Systems* (ICSGTEIS), pp. 13-18. https://doi.org/10.1109/ICSGTEIS.2018.8709108

Sathish, C., Chidambaram, I.A., & Manikandan, M. (2023). Switched Z-Source Boost Converter in Hybrid Renewable Energy System for Grid-Tied Applications. *Journal of Electrical Systems*, *1*(19), 64-81.

Sathish, C., University, A., Chidambram, I.A., & Manikandan, M. (2022). Reactive Power Compensation in a Hybrid Renewable Energy System through Fuzzy Based Boost Converter. *Problemele Energeticii Regionale*, *1*, 10-26. https://doi.org/10.52254/1857-0070.2022.1-53.02

Sathish, C., University, A., Chidambram, I.A., & Manikandan, M. (2023). Hybrid Renewable Energy System with High Gain Modified Z-Source Boost Converter for Grid-Tied Applications, *Problemele Energeticii Regionale*, *1*(57), 39-54. https://doi.org/10.52254/1857-0070.2023.1-57.04

Sindi, H.F., Alghamdi, S., Rawa, M., Omar, A.I., & Elmetwaly, A.H. (2023). Robust control of adaptive power quality compensator in Multi-Microgrids for power quality enhancement using puzzle optimization algorithm. *Ain Shams Engineering Journal*, *14*(8), 102047. https://doi.org/10.1016/j.asej.2022.102047

Thota, P.K., Somaskandan, G., & Mani, M. (2023). The Voltage stability analysis for grid-connected PV system using optimized control tested by IEEE 14 &30 bus system, International *Journal of Experimental Research and Review*, *30*, 109-118. https://doi.org/10.52756/ijerr.2023.v30.012

Quawi, A., Shuaib, Y.M., & Manikandan, M. (2023). Power Quality Improvement Using ANN Controller For Hybrid Power Distribution Systems. *Intelligent Automation & Soft Computing*, *36*(3), 3469-3486. https://doi.org/10.32604/iasc.2023.035001

How to cite this Article:

Rudraram Ramesh, Chinnathambi Sasi and Mani Manikandan (2023). An efficient PV-integrated UPQC system for power quality enhancement using improved Chicken swarm optimization. *International Journal of Experimental Research and Review*. *33*, 57-70.

DOI: https://doi.org/10.52756/ ijerr.2023.v33spl.006